

Study of Higgs \rightarrow invisible using kinematic fit method applied jet energy resolution of ILD

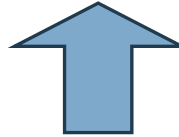
Yu Kato
The Univ. of Tokyo

Goal of this study

Improve analysis performance



kinematic fit



apply jet energy resolution

Flow of study

Evaluate jet energy resolution

ILD model : ILD_I(s)5_v02

➤ jet energy & $\cos \theta$ dependence

evaluate jet angle resolution → apply to kinematic fit

kinematic fit

use MarlinKinfit - fitter engine : OPALFitter

apply jet resolution

➤ check effect & accuracy of fit

Improve analysis performance

[BSM search using Higgs \rightarrow invisible]

Setting of Evaluation JER

- ILCSoft : v01-19-05 (gcc49)
- ILDConfig : v01-19-05-p01
- ILD models : ILD_I5_o1_v02, ILD_s5_o1_v02
- samples : Z→uds (/hsm/ilc/grid/storm/prod/ilc/mc-opt.dsk/ild/dst/calib/uds/*)

\sqrt{s} [GeV]	30	40	60	91	120	160	200	240	300	350	400	500
I5 [events]	10k	9k	10k	9k	10k							
s5 [events]	10k	10k	10k	10k	9k	10k	10k	9k	10k	10k	10k	10k

- jet resolution definition
 - use RMS₉₀ method
 - Energy

Update.

$$\frac{\sigma_E}{E} = \frac{\text{RMS}_{90}(E_j)}{\text{mean}_{90}(E_j)} = \sqrt{2} \frac{\text{RMS}_{90}(E_{jj})}{\text{mean}_{90}(E_{jj})}$$

(J. S. Marshall and M. A. Thomson, "Pandora Particle Flow Algorithm", [arXiv:1308.4537](https://arxiv.org/abs/1308.4537) [physics.ins-det])

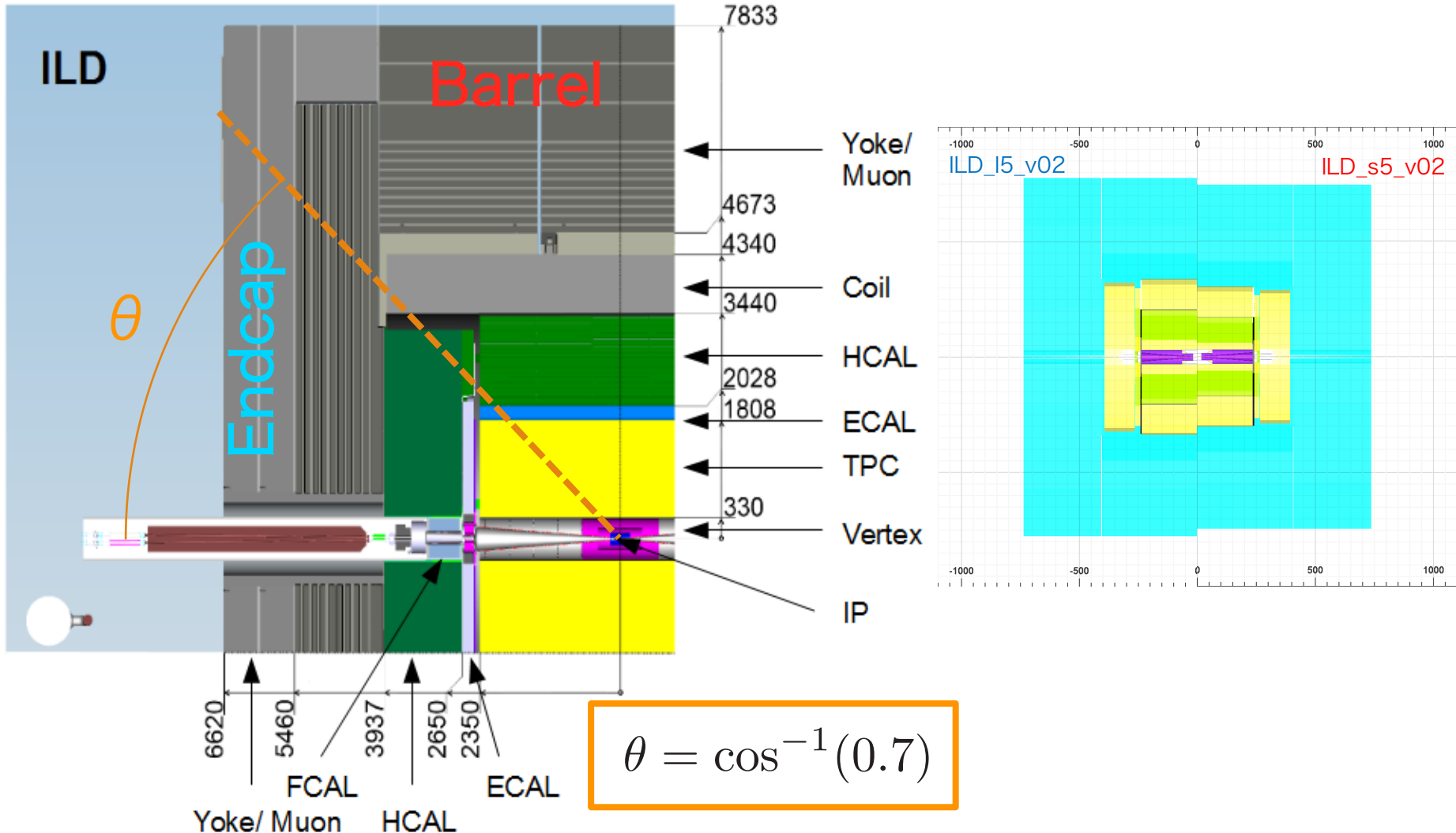
- Angle
 - use jet clustering: Durham

$$\delta\phi = \text{RMS}_{90}(\phi_{rec} - \phi_{mc})$$

$$\delta\theta = \text{RMS}_{90}(\theta_{rec} - \theta_{mc})$$

Evaluate JER

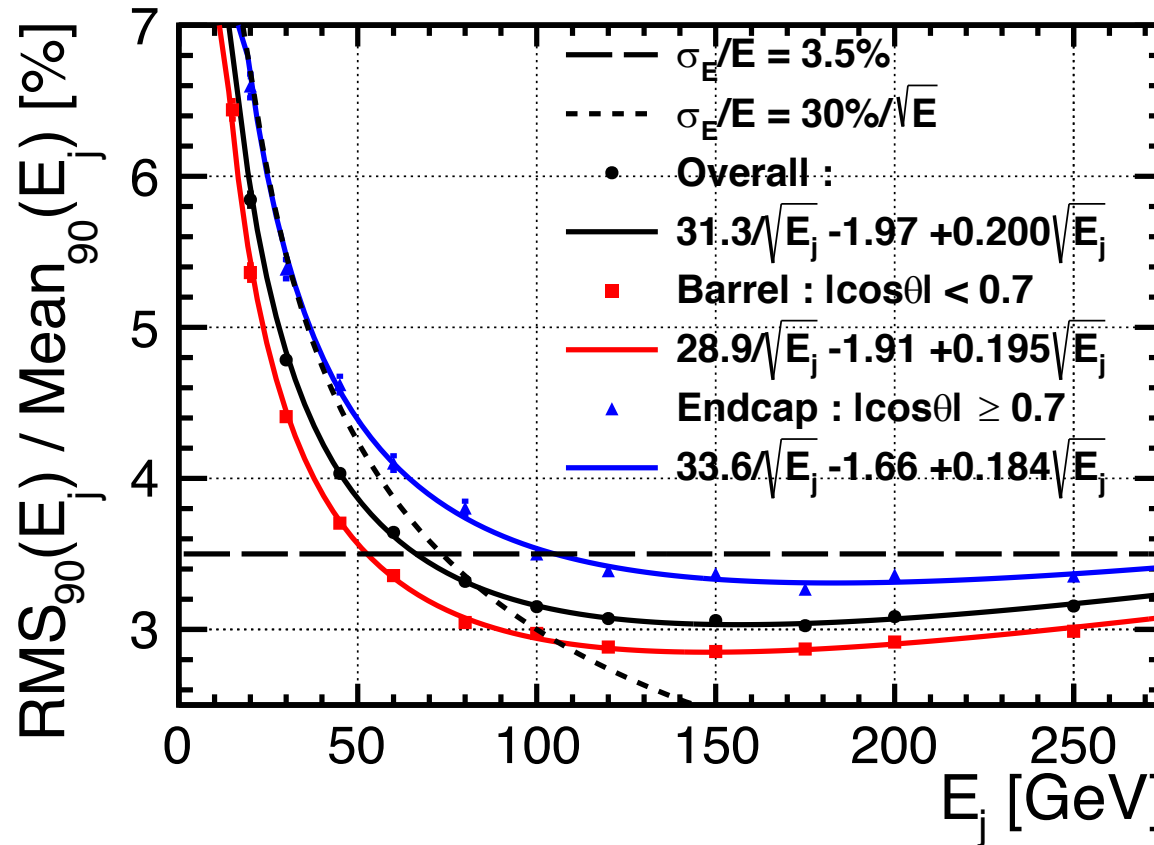
ILD model Detailed Baseline Design



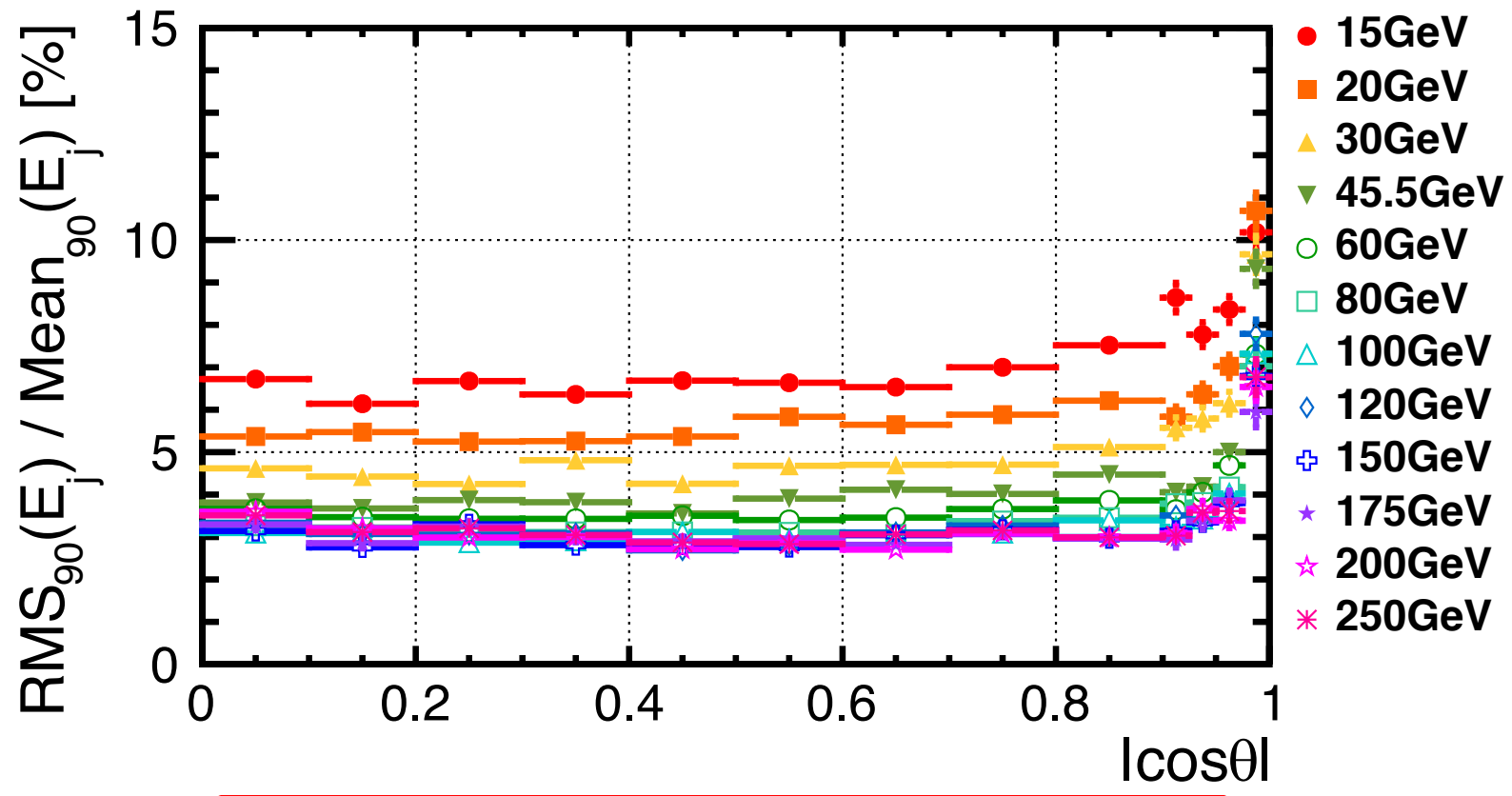
Result : Energy dependence

$$\frac{\sigma_E}{E} = \frac{\alpha}{\sqrt{E}} \oplus \beta(E)$$

sv01-19-05.mILD_I5_o1_v02_nobg



Result : energy & angle dependence

sv01-19-05.mILD_I5_o1_v02_nobg**apply this result to kinematic fit**

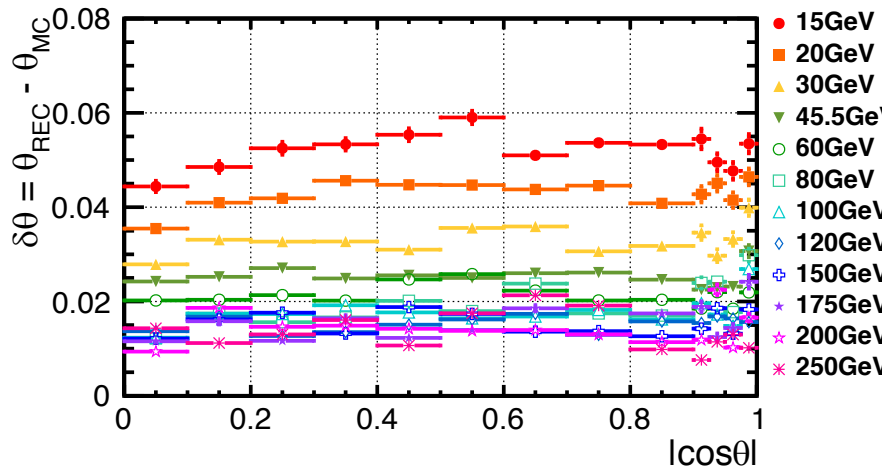
Evaluate JER

Angular resolution

polar angle

$$\delta\theta = RMS_{90}(\theta_{rec} - \theta_{mc})$$

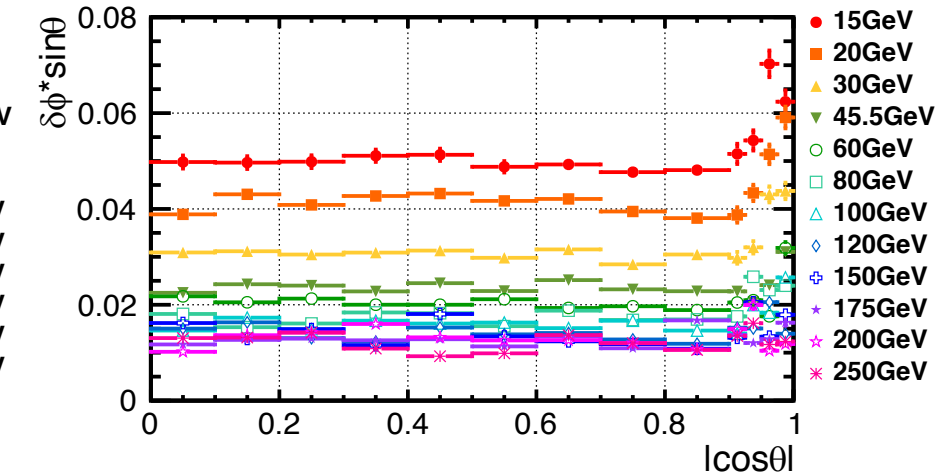
sv01-19-05.mILD_I5_o1_v02_nobg



azimuth angle

$$\delta\phi * sin\theta = RMS_{90}\{(\phi_{rec} - \phi_{mc})sin\theta\}$$

sv01-19-05.mILD_I5_o1_v02_nobg



For evaluation of angular resolution,
use jet clustering.

Durham algorithm

$$y_{ij} = \frac{2\min(E_i^2, E_j^2)(1 - \cos\theta_{ij})}{Q^2}$$

apply this result to kinematic fit

Principle of kinematic fit

seek minimum of $\chi_T^2(\vec{\eta}, \vec{\xi}, \vec{\lambda})$
under kinematic constraints

$$\chi_T^2(\vec{\eta}, \vec{\xi}, \vec{\lambda}) = \chi^2(\vec{\eta}) + F_C(\vec{\eta}, \vec{\xi}, \vec{\lambda})$$

$$\chi^2(\vec{\eta}) = (\vec{\eta} - \vec{y})^T V^{-1} (\vec{\eta} - \vec{y})$$

$$F_C(\vec{\eta}, \vec{\xi}, \vec{\lambda}) = 2\vec{\lambda}^T \cdot \vec{f}(\vec{\eta}, \vec{\xi})$$

method of Lagrange multipliers

$$\left\{ \begin{array}{l} \frac{1}{2} \frac{\partial \chi_T^2}{\partial \eta_i} = V_{ij}^{-1} (\eta_j - y_j) + \frac{\partial f_k}{\partial \eta_i} \lambda_k = 0 \quad (i = 1, \dots, N) \\ \frac{1}{2} \frac{\partial \chi_T^2}{\partial \xi_i} = \frac{\partial f_k}{\partial \xi_i} \lambda_k = 0 \quad (i = 1, \dots, J) \\ \frac{1}{2} \frac{\partial \chi_T^2}{\partial \lambda_i} = f_i = 0 \quad (i = 1, \dots, K) \end{array} \right.$$

$$\text{d.o.f. : } N_{dof} = N_m - \{N_f - (K - J)\} = K - J$$

\vec{y} : measured values (N)

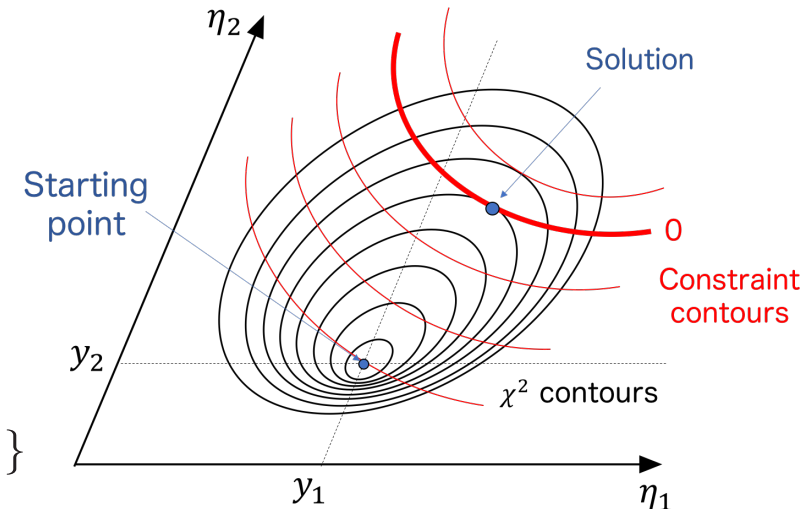
$\vec{\eta}$: fit parameters (N)

$\vec{\xi}$: unmeasured parameters (J)

$\vec{\lambda}$: Lagrange multipliers (K)

\vec{f} : constraint functions (K)

V : covariance matrix ($N \times N$)

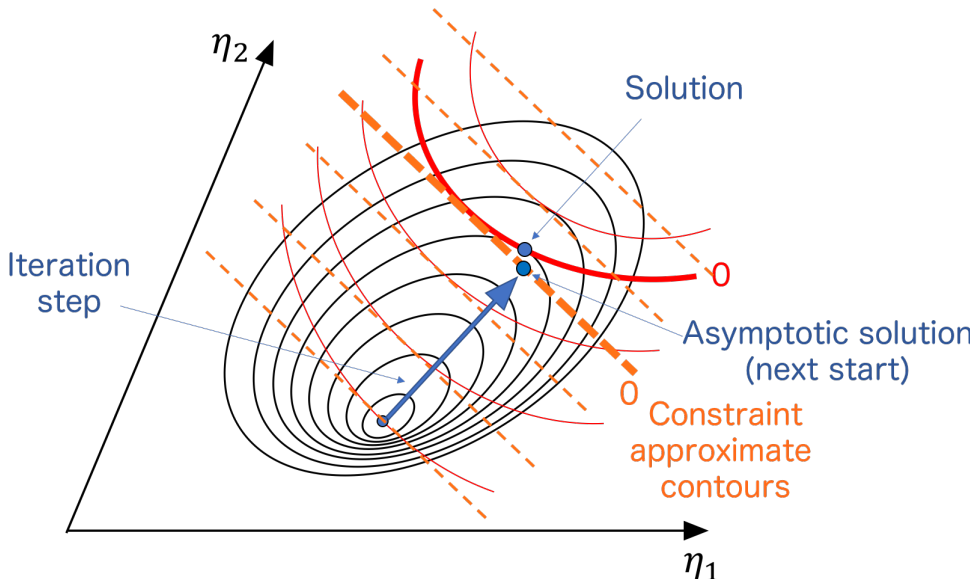


MarlinKinfit : OPALFitter

For iterative solution : Taylor-expansion of the constraints

$$f_i(\vec{\eta}^{\nu+1}, \vec{\xi}^{\nu+1}) = f_i(\vec{\eta}^\nu, \vec{\xi}^\nu) + \frac{\partial f_i}{\partial \eta_j} \Big|_{\eta_j=\eta_j^\nu} (\eta_j^{\nu+1} - \eta_j^\nu) + \frac{\partial f_i}{\partial \xi_k} \Big|_{\xi_k=\xi_k^\nu} (\xi_k^{\nu+1} - \xi_k^\nu)$$

$$\left\{ \begin{array}{l} V_{ij}^{-1}(\eta_j^{\nu+1} - y_j) + \frac{\partial f_k}{\partial \eta_i} \Big|_{\eta_i=\eta_i^\nu} \lambda_k^{\nu+1} = 0 \quad (i = 1, \dots, N) \\ \frac{\partial f_k}{\partial \xi_i} \Big|_{\xi_i=\xi_i^\nu} \lambda_k^{\nu+1} = 0 \quad (i = 1, \dots, J) \\ f_i(\vec{\eta}^{\nu+1}, \vec{\xi}^{\nu+1}) = 0 \quad (i = 1, \dots, K) \end{array} \right.$$

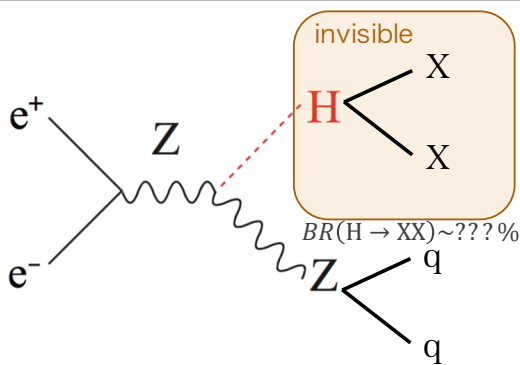


Convergence condition

- ✓ $\delta\chi^2 < 0.01\% \cap \delta F_C < 10^{-3}$
 $\cap F_C < 10^{-2} \cdot \chi^2$
- or
- ✓ all $f_i < 10^{-6} \cap \delta(\eta, \xi, \lambda) < 10^{-6}$

kinematic fit

ZH processor



□ Z mass constraint

$$m_{jj} = m_Z = 91.2 \text{ GeV}$$

□ jet mass constraint

$$m_j^{\text{before}} = m_j^{\text{after}}$$

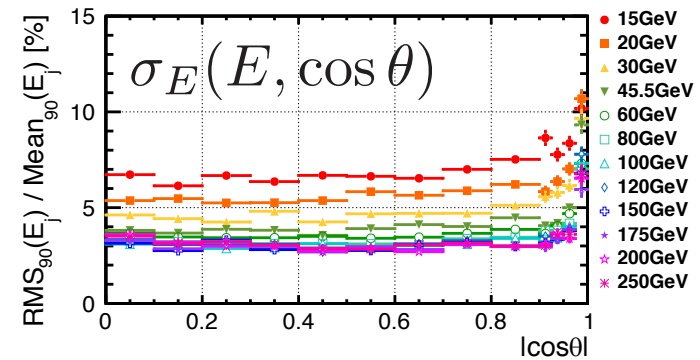
□ Implement of jet resolution

$$\sigma_E(E, \cos \theta), \sigma_\theta(E, \cos \theta), \sigma_\phi(E, \cos \theta)$$

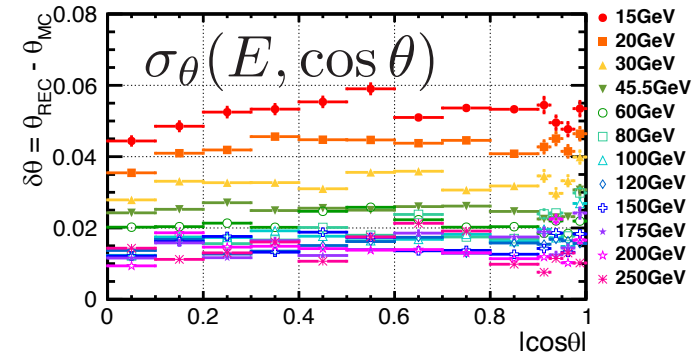
□ degrees of freedom

$$\begin{aligned} N_{\text{dof}} &= N_m - \{N_f - (K - J)\} \\ &= K - J = 1 \end{aligned}$$

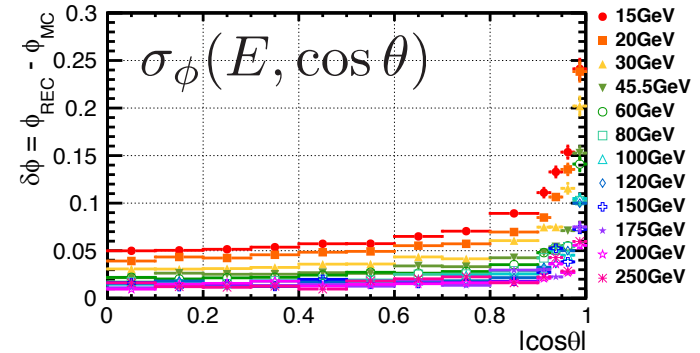
sv01-19-05.mILD_l5_o1_v02_nobg



sv01-19-05.mILD_l5_o1_v02_nobg

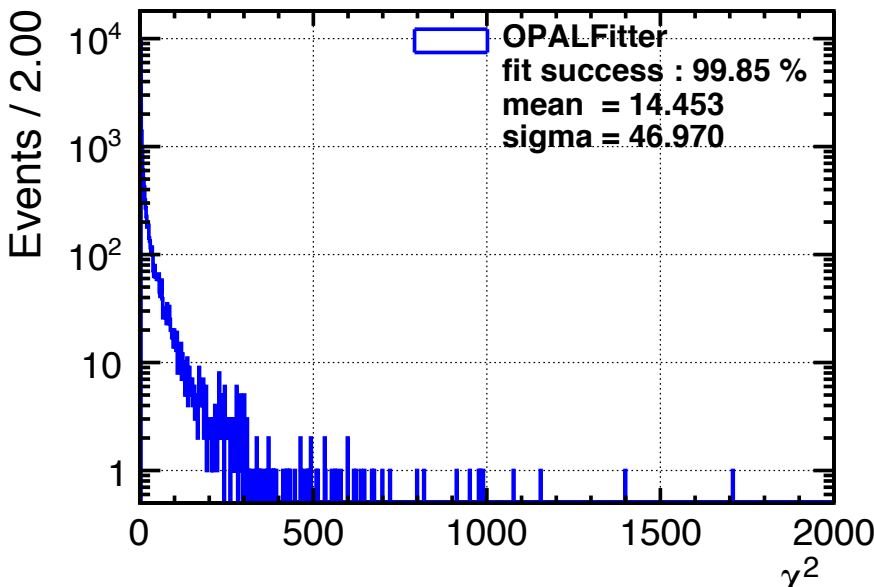


sv01-19-05.mILD_l5_o1_v02_nobg



Result : accuracy of fit

sv01-19-05.mILD_o1_v05.eL.pR



χ^2 distribution

Mean : 14.5

Ndof : 1

Mean > Ndof

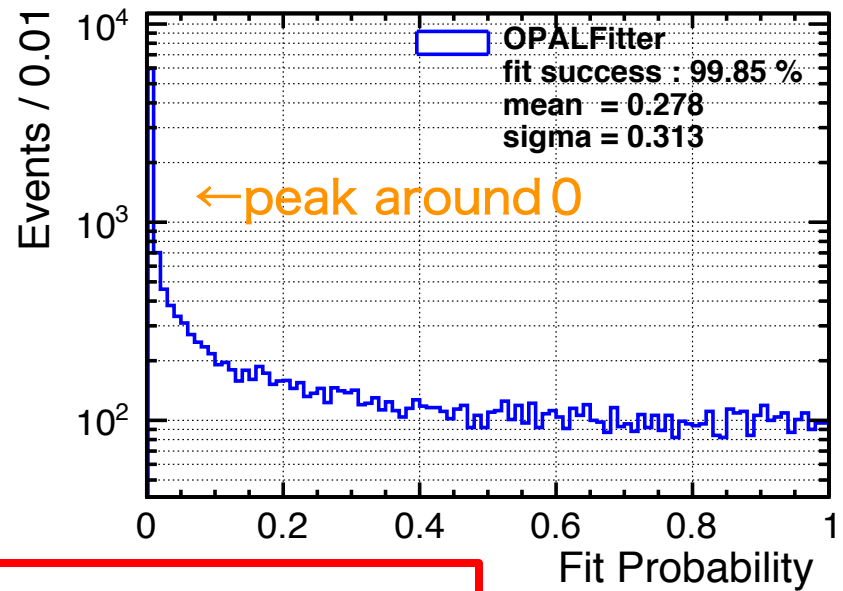
fit probability

$$= \int_{\chi^2_{result}}^{\infty} f_{\chi^2}(\chi^2; \nu) d\chi^2$$

fit with well-estimated errors

→ normal distributed between 0 and 1

sv01-19-05.mILD_o1_v05.eL.pR



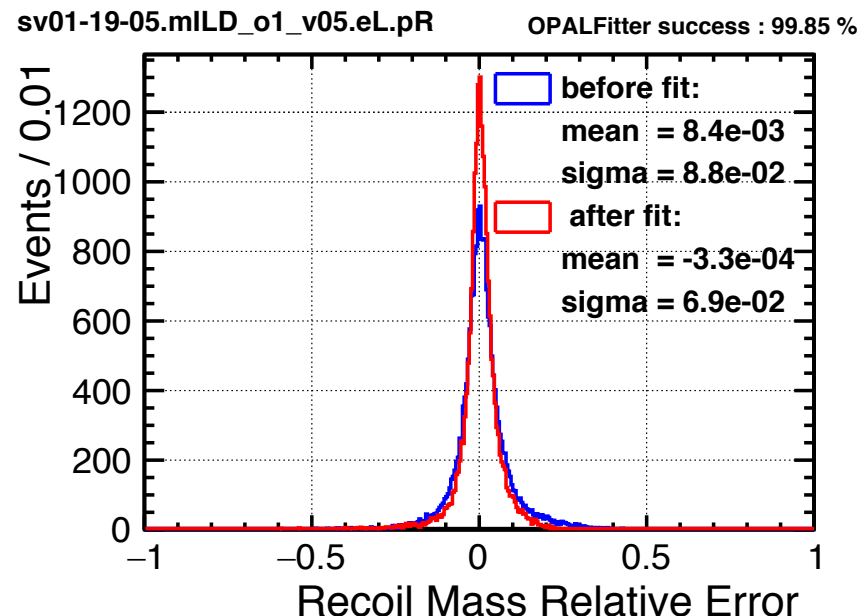
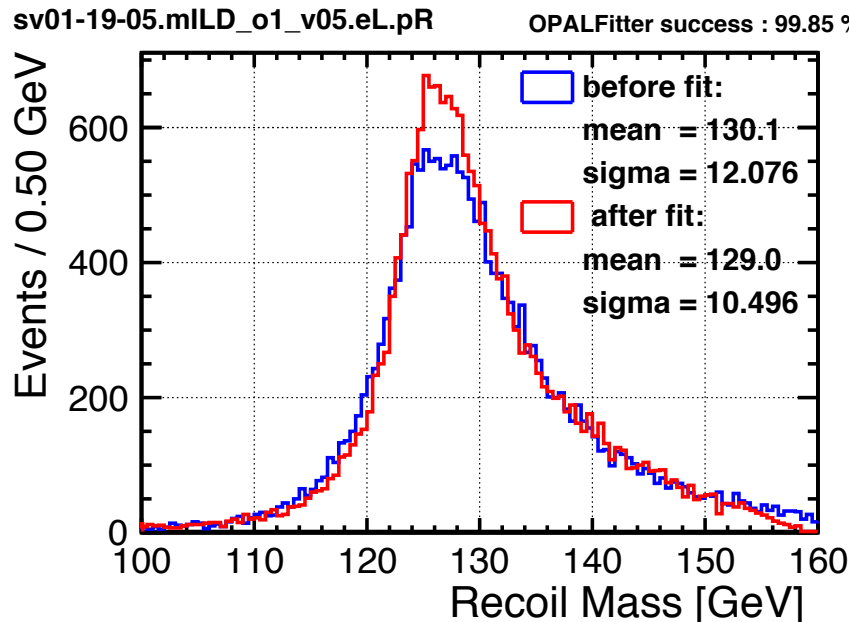
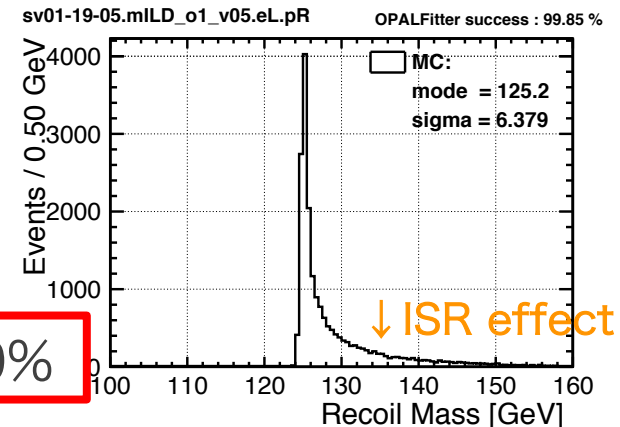
a possibility of underestimating parameter error

Result : Recoil mass

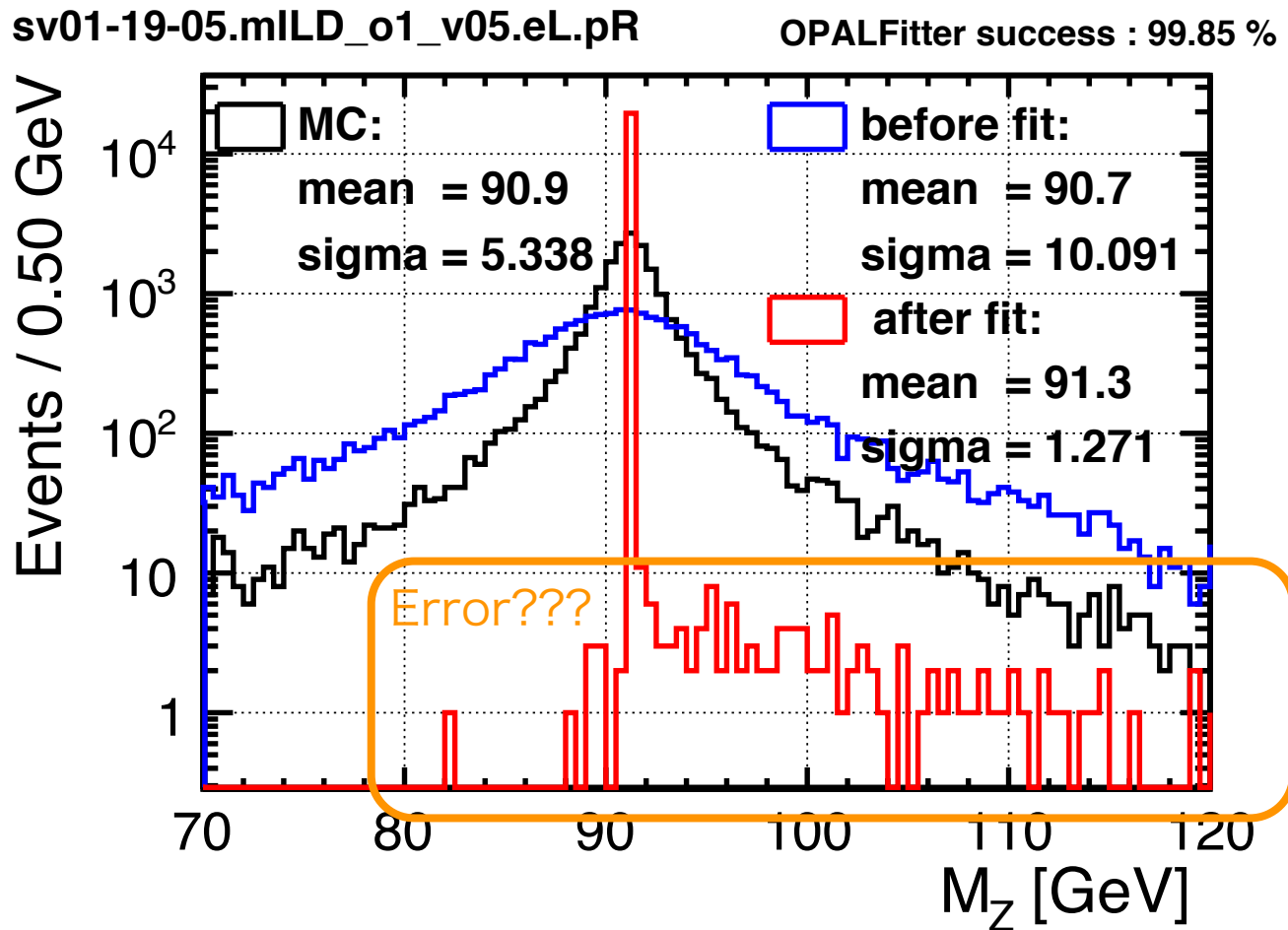
$$M_{rec} = \sqrt{(\sqrt{s} - E_Z)^2 - |\vec{p}_Z|^2}$$

$$\delta M_{rec} = \frac{M_{rec}^{result} - M_{rec}^{mc}}{M_{rec}^{mc}}$$

improve recoil mass resolution ~20%



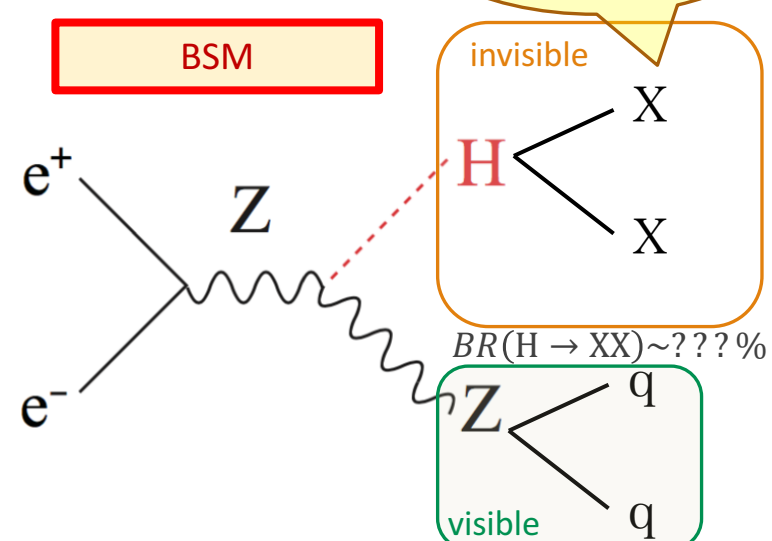
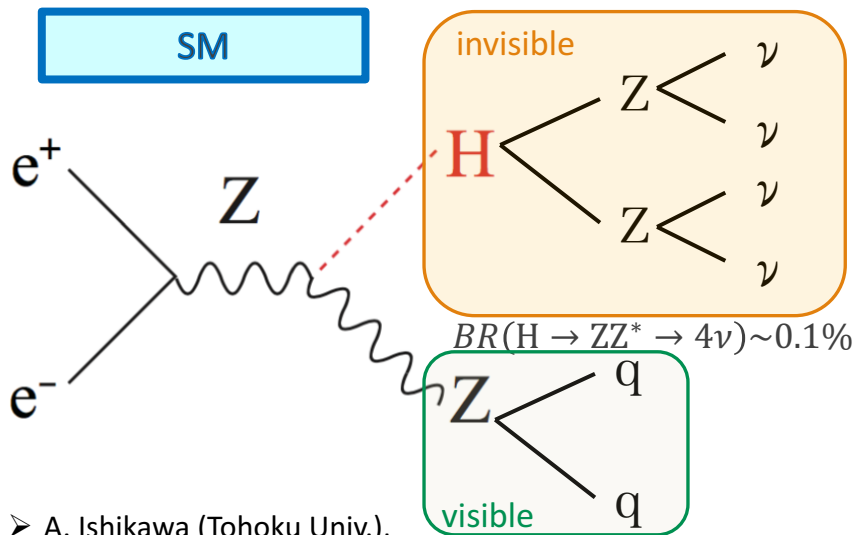
Problems : Z mass distribution



Motivation

- In SM, Higgs decays invisibly through $H \rightarrow ZZ^* \rightarrow 4\nu$ ($\text{BR}(H \rightarrow \text{inv.}) \sim 0.1\%$)
- If $\text{BR}(H \rightarrow \text{inv.})$ exceeds SM prediction, it signifies new physics beyond SM (BSM)
- We estimate SM upper limit of $\text{BR}(H \rightarrow \text{inv.})$
- Compare between left & right polarization at the ILC

Previous study (A.Ishikawa)
(95% CL, 250fb^{-1})
left pol. : right pol.
0.95% : 0.69%



➤ A. Ishikawa (Tohoku Univ.),
"Search for Invisible Higgs Decays at the ILC" LCWS2014@Belgrade

Higgs→invisible

Cut table $(P_{e^-}, P_{e^+}) = (-0.8, +0.3)$

カット条件	有意度	信号事象	全背景事象	ZZ	WW	$\nu\nu Z$	other bkg
No Cut	0.84	5255	3.93×10^7	214211	2748230	67952	3.63×10^7
$N_{lep} = 0$	1.00	5249	2.74×10^7	165399	1276030	67853	2.59×10^7
Pre-Cut	7.54	5026	439363	35027	69535	33852	300949
$N_{pfo} > 15 \& N_{charged} > 6$	9.66	4947	256873	34332	67457	33236	121848
$p_{T,jj} \in (20, 80)\text{GeV}$	12.48	4688	136149	30207	56149	29166	20627
$M_{jj} \in (80, 100)\text{GeV}$	13.50	3919	80266	23533	29210	23675	3848
$ \cos\theta_{jj} < 0.9$	13.94	3768	69199	20457	24817	21246	2679

w/o kinematic fit

カット条件	有意度	信号事象	全背景事象	ZZ	WW	$\nu\nu Z$	other bkg
共通部分	13.94	3768	69199	20457	24817	21246	2679
$M_{recoil} \in (100, 160)\text{GeV}$	13.95	3765	69002	20438	24748	21174	2642
BDT > -0.0718	15.54	3388	44086	12604	14941	14676	1865

w/ kinematic fit

カット条件	有意度	信号事象	全背景事象	ZZ	WW	$\nu\nu Z$	other bkg
共通部分	13.94	3768	69199	20457	24817	21246	2679
$M_{recoil} \in (100, 160)\text{GeV}$	15.10	3766	58404	15873	21289	18665	2577
BDT > -0.0867	16.26	3425	40893	11086	14030	13903	1874

Higgs→invisible

Cut table $(P_{e^-}, P_{e^+}) = (+0.8, -0.3)$

カット条件	有意度	信号事象	全背景事象	ZZ	WW	$\nu\nu Z$	other bkg
No Cut	0.76	3549	2.16×10^7	116792	189591	23127	2.13×10^7
$N_{lep} = 0$	0.95	3545	1.39×10^7	89111	88065	23092	1.37×10^7
Pre-Cut	7.33	3391	210605	16373	4918	8970	180344
$N_{pfo} > 15 \& N_{charged} > 6$	10.03	3331	106837	16028	4773	8786	77250
$p_{Tjj} \in (20, 80)\text{GeV}$	15.59	3144	37369	14018	4022	7793	11536
$M_{jj} \in (80, 100)\text{GeV}$	17.17	2632	20815	10828	2087	6121	1779
$ \cos\theta_{jj} < 0.9$	17.81	2535	17670	9387	1806	5373	1104

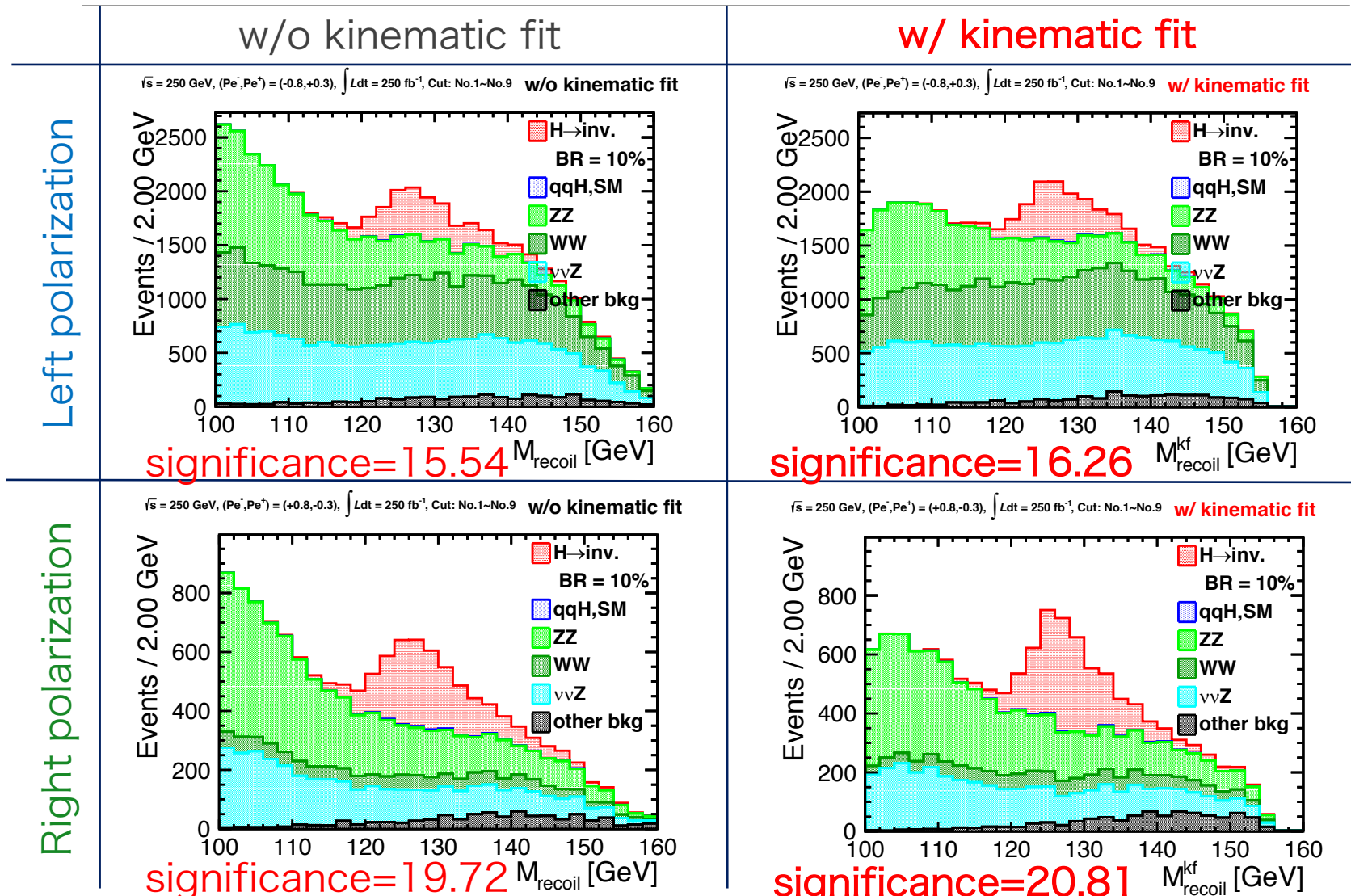
w/o kinematic fit

カット条件	有意度	信号事象	全背景事象	ZZ	WW	$\nu\nu Z$	other bkg
共通部分	17.81	2535	17670	9387	1806	5373	1104
$M_{recoil} \in (100, 160)\text{GeV}$	17.83	2532	17598	9376	1800	5366	1056
BDT > -0.0840	19.72	2298	11231	5800	1170	3463	798

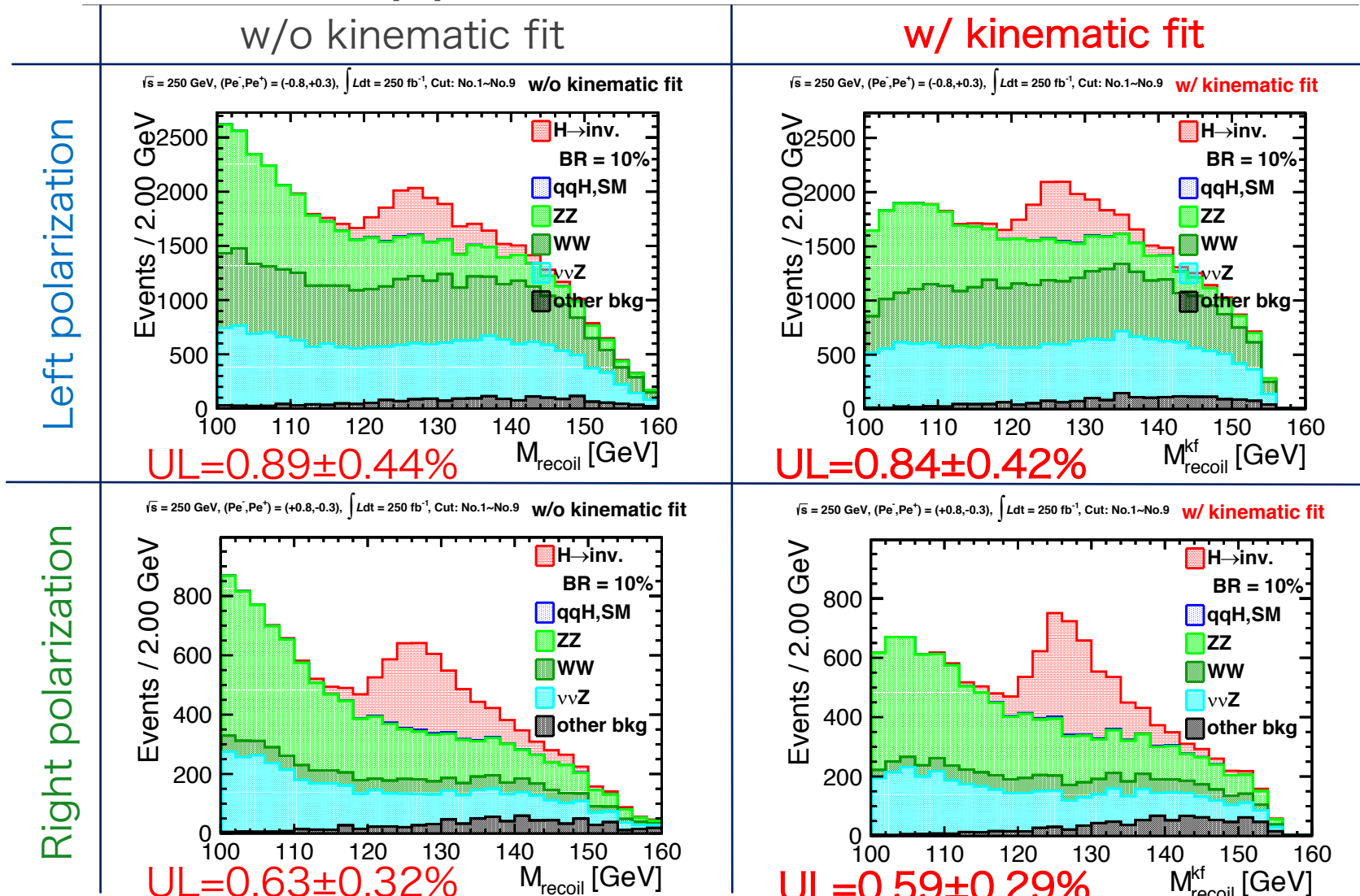
w/ kinematic fit

カット条件	有意度	信号事象	全背景事象	ZZ	WW	$\nu\nu Z$	other bkg
共通部分	17.81	2535	17670	9387	1806	5373	1104
$M_{recoil} \in (100, 160)\text{GeV}$	19.61	2533	14104	7196	1549	4274	1085
BDT > -0.1162	20.81	2395	10806	5431	1187	3318	870

Result : Recoil mass distribution



Result : Upper limit of BR (95% CL)



backup

今後の課題

ジェットエネルギー分解能評価

- エンドキャップ部分のより精細な評価 ← 統計量の増加
- cジェット、bジェット評価の追加
- ジェットクラスタリングを用いた評価： $E_{j1} \neq E_{j2}$
- ジェット質量(または運動量)依存性の追加

kinematic fit

- フィッティング精度の改善：分解能をスケールする
- soft constraintの実装：Zボソンの自然幅を考慮
- 他の物理過程への応用

Higgs→invisible崩壊分岐比の上限推定

- 反跳質量以外のフィット後の変数を事象選別に使用
- 推定に用いる反跳質量領域の最適化
- より高度な手法を用いて上限評価
 - ex.) profile likelihood ratio

まとめ

ジェットエネルギー分解能評価

ILDモデルのシミュレーションを行い
ジェットエネルギー分解能を評価した
エネルギー&角度依存性の精査
角度分解能も同様に評価を行った

kinematic fit 構築

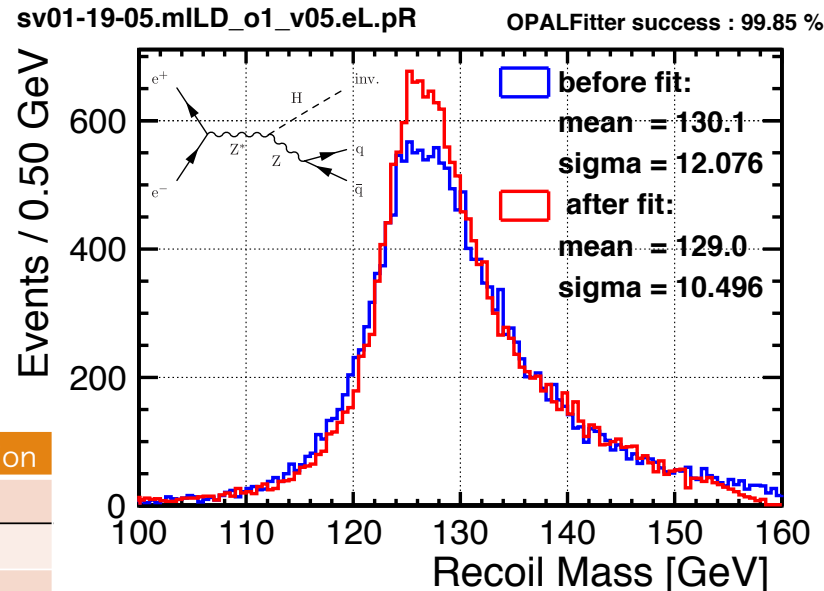
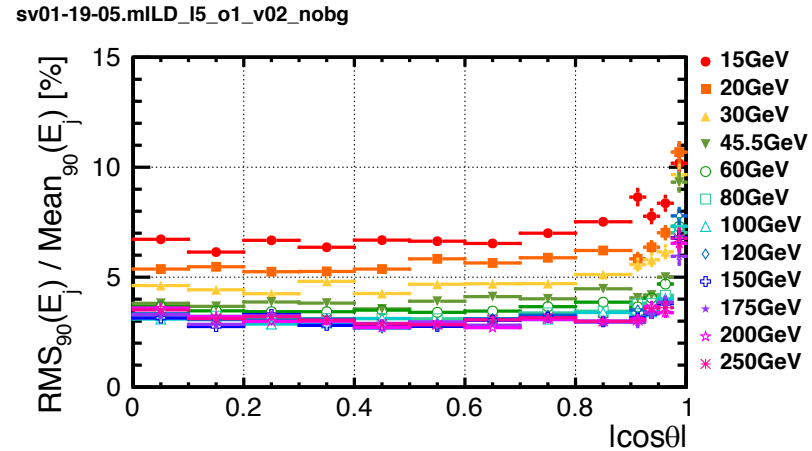
ジェット分解能を実装したkinematic fitを構築した

kinematic fitに必要なパラメータ誤差を
ジェット分解能評価の結果↑から取得
Higgs→invisible過程の反跳質量分解能が
~20%改善した

実際の解析へ応用

Higgs→invisible崩壊分岐比の上限推定に
応用し、kinematic fitによる効果を確認

UL of BR [%] (95%CL)	Left polarization	Right polarization
Previous study	0.95	0.69
w/o kinematic fit	0.89 ± 0.44	0.63 ± 0.32
w/ kinematic fit	0.84 ± 0.42	0.59 ± 0.29



動機

- 標準理論下でヒッグスは以下の反応でのみinvisible崩壊をする
 $H \rightarrow ZZ^* \rightarrow 4\nu$ ($BR(H \rightarrow \text{inv.}) \sim 0.1\%$)
- 崩壊分岐比 $BR(\text{Higgs} \rightarrow \text{invisible})$ に有意な超過
→ 新物理が存在する確たる証拠
- $BR(\text{Higgs} \rightarrow \text{invisible})$ の95% CL 上限を推定したい
- ILCにおける2種類のビーム偏極モード下での結果を比較

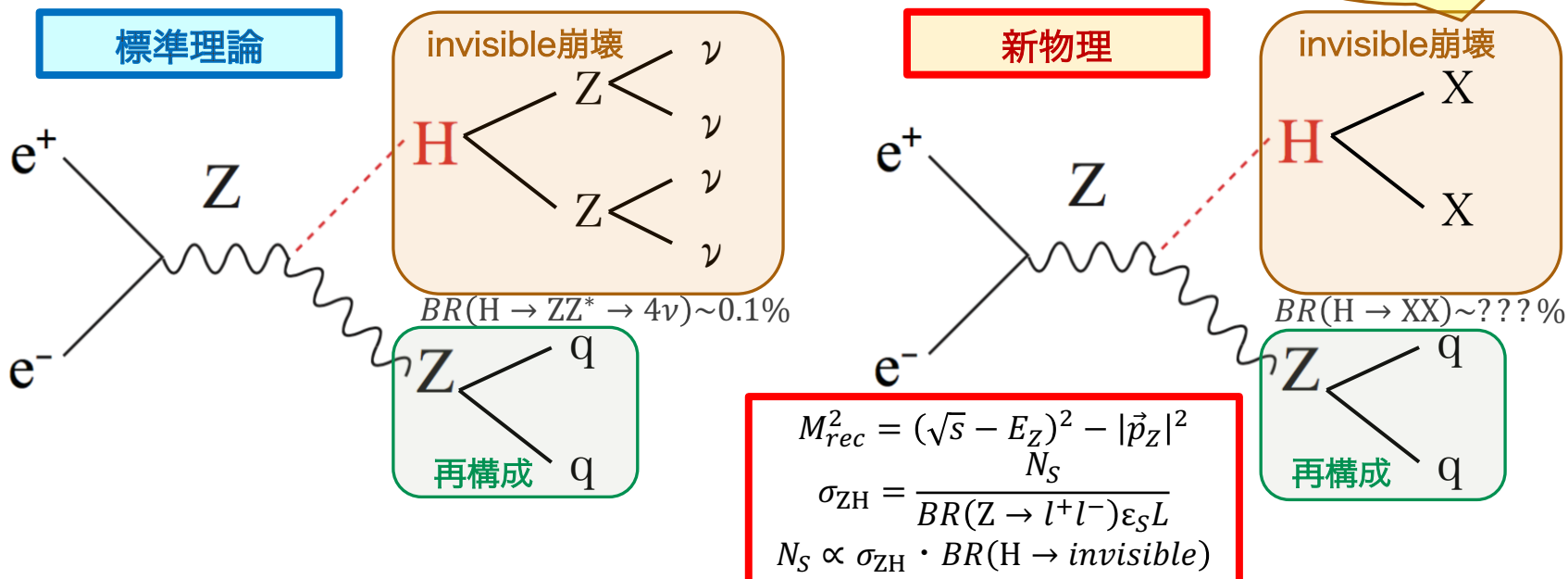
先行研究の結果

(A.Ishikawa)

(95% CL, 250fb^{-1})

left pol. : right pol.
0.95% : 0.69%

暗黒物質?
超対称性粒子?

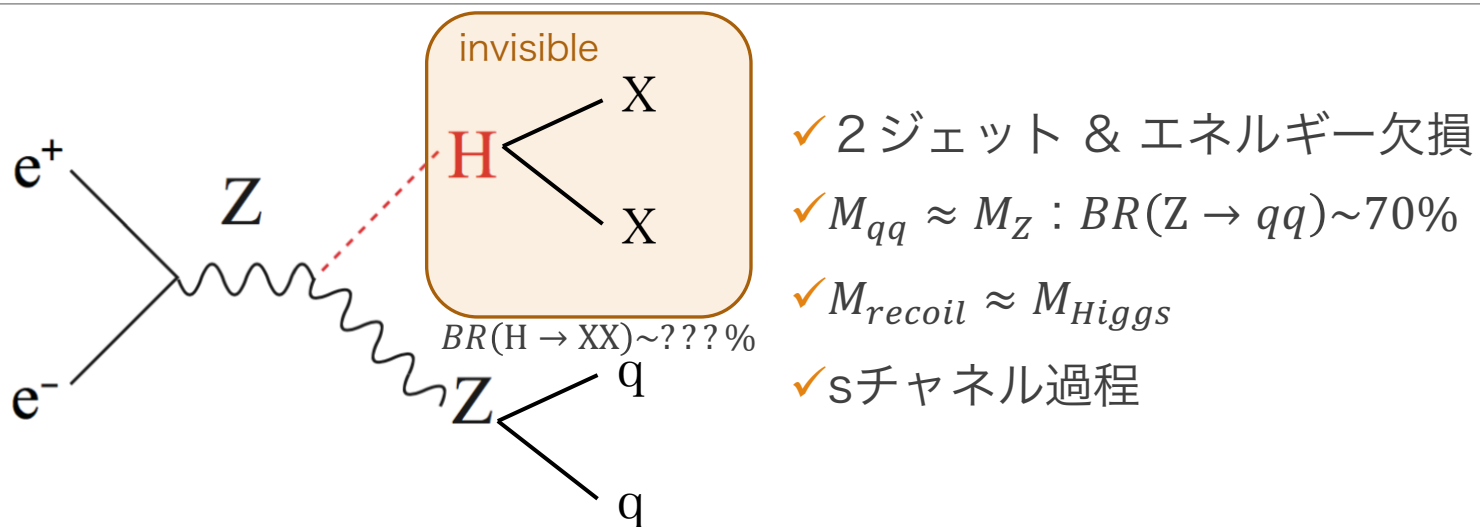


➤ A. Ishikawa (Tohoku Univ.),

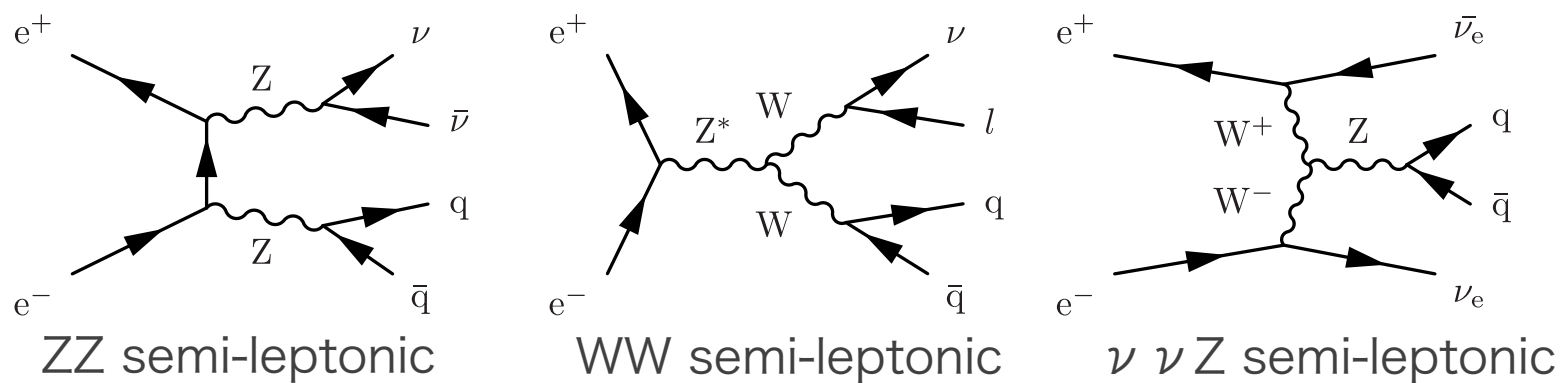
"Search for Invisible Higgs Decays at the ILC" LCWS2014@Belgrade

反跳質量測定法

信号事象の特徴



主要な背景事象



解析

● シミュレーション条件

- Generator: WHIZARD 1.95
- Samples: DBD sample + Dirac sample ($e^+e^- \rightarrow qqH, H \rightarrow ZZ^* \rightarrow 4\nu$)
- Detector: ILD full simulation (ILD_o1_v05)
- $\sqrt{s} = 250 \text{ GeV}$, $\int L dt = 250 \text{ fb}^{-1}$, $(P_{e^-}, P_{e^+}) = (-0.8, +0.3), (+0.8, -0.3)$
“Left” “Right”

● 解析の流れ

1. 粒子再構成：“PandoraPFA”

- Isolated lepton tag : 高いエネルギー運動量をもつレプトンを含む事象の除去

2. ジェット クラスタリング：“Durham algorithm”

- すべての事象に対して、ハドロンを2本のジェットにまとめあげる

3. kinematic fit

- MarlinKinfitを使用 : OPALFitter, $M_{jj} = M_Z$, $M_{j,before} = M_{j,after}$

4. 事象選別(次ページに詳細)

- $\text{BR}(H \rightarrow \text{invisible}) = 10\%$ を仮定

5. 崩壊分岐比の上限推定

- $\text{BR}(H \rightarrow \text{invisible}) = [1\sim10\%]$ のテンプレートを用意し、95% CLの上限を推定

Summary

Evaluation of JER kinematic fit

ジェット分解能を実装したkinematic fitを構築した

kinematic fitに必要なパラメータ誤差をジェット分解能評価の結果↑から取得

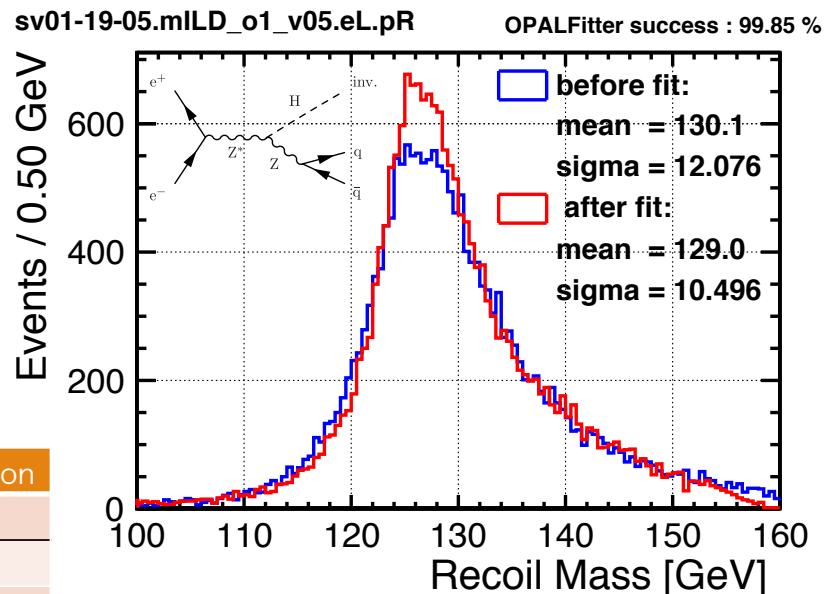
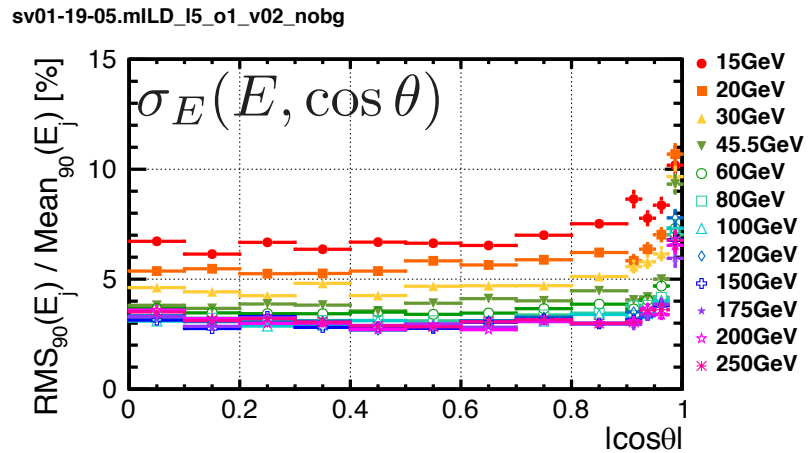
Higgs→invisible過程の反跳質量分解能が~20%改善した

Higgs→invisible

Estimate upper limit of $\text{BR}(\text{H} \rightarrow \text{inv.})$

Check effect by kinematic fit

UL of BR [%] (95%CL)	Left polarization	Right polarization
Previous study	0.95	0.69
w/o kinematic fit	0.89 ± 0.44	0.63 ± 0.32
w/ kinematic fit	0.84 ± 0.42	0.59 ± 0.29

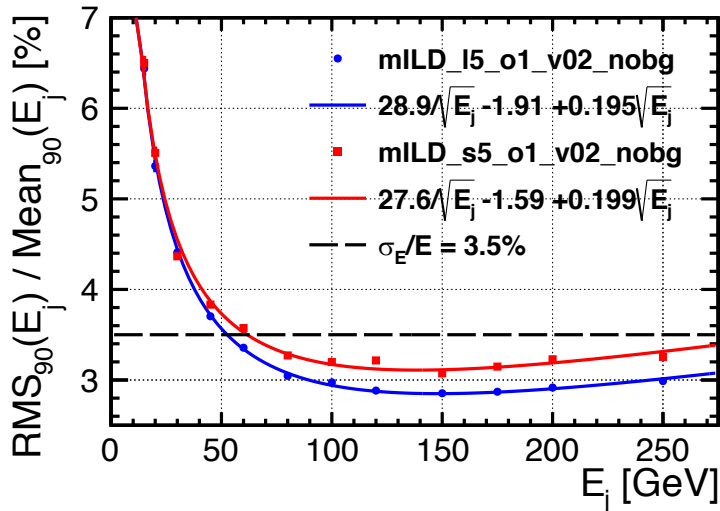


List of envelope parameters for ILD_I5_v02						
detector	inner radius	outer radius	half length min z, max z	additional parameters		
VXD	15.0	101.0	177.6	VXD_cone_min_z VXD_cone_max_z VXD_inner_radius_1	80.0 150.0 25.1	
FTD	37.0	309.0	2350.0	FTD_outer_radius_1 FTD_outer_radius_2 FTD_min_z_0 FTD_min_z_1 FTD_min_z_2 FTD_cone_min_z FTD_cone_radius	152.8 299.7 177.7 368.2 644.2 230.0 192.0	
SIT	152.9	324.6	644.1	SIT_outer_radius_1 SIT_half_length_1	299.8 368.1	
TPC	329.0	1769.8	2350.0			
SET	1769.9	1804.3	2350.0			
Ecal	1804.8	2028.0	2350.0	Ecal_Hcal_symmetry Ecal_symmetry	8 8	
EcalEndcap	400.0	2095.84	2411.8, 2635.0	EcalEndcap_symmetry	8	
EcalEndcapRing	250.0	390.0	2411.8, 2635.0			
Hcal	2058.0	3395.5	2350.0	Hcal_inner_symmetry	8	
HcalEndcap	350.0	3225.5	2650.0, 3937.0			
HcalEndcapRing	2145.84	2980.0	2411.8, 2635.0	HcalEndcapRing_symmetry	8	
Coil	3425.0	4175.0	3872.0			
Yoke	4475.0	7776.0	4047.0	Yoke_symmetry	12	
YokeEndcap	300.0	7776.0	4072.0, 7373.0	YokeEndcap_symmetry	12	
YokeEndcapPlug	300.0	3395.54	3937.2, 4072.0	YokeEndcapPlug_symmetry	12	
BeamCal	17.8	140.0	3115.0, 3315.0	BeamCal_thickness	200.0	
LHCal	130.0	315.0	2680.0, 3160.0	LHCal_thickness	480.0	
LumiCal	80.0	202.1	2411.8, 2540.5	LumiCal_thickness	128.7	

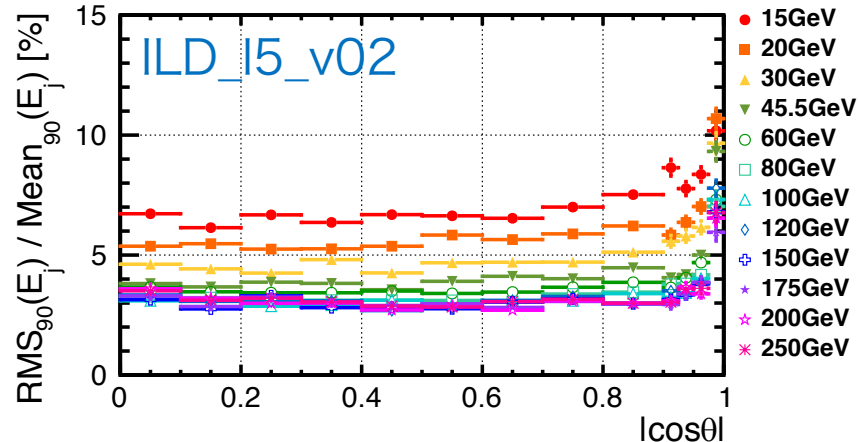
List of envelope parameters for ILD_s5_v02						
detector	inner radius	outer radius	half length min z, max z	additional parameters		
VXD	15.0	101.0	177.6	VXD_cone_min_z VXD_cone_max_z VXD_inner_radius_1	80.0 150.0 25.1	
FTD	37.0	309.0	2350.0	FTD_outer_radius_1 FTD_outer_radius_2 FTD_min_z_0 FTD_min_z_1 FTD_min_z_2 FTD_cone_min_z FTD_cone_radius	152.8 299.7 177.7 368.2 644.2 230.0 192.0	
SIT	152.9	324.61	644.1	SIT_outer_radius_1 SIT_half_length_1	299.8 368.1	
TPC	329.0	1426.8	2350.0			
SET	1426.9	1461.3	2350.0			
Ecal	1461.8	1685.0	2350.0	Ecal_Hcal_symmetry Ecal_symmetry	8 8	
EcalEndcap	400.0	1717.92	2411.8, 2635.0	EcalEndcap_symmetry	8	
EcalEndcapRing	250.0	390.0	2411.8, 2635.0			
Hcal	1715.0	3045.83	2350.0	Hcal_inner_symmetry	8	
HcalEndcap	350.0	2875.83	2650.0, 3937.0			
HcalEndcapRing	1767.92	2656.92	2411.8, 2635.0	HcalEndcapRing_symmetry	8	
Coil	3075.33	3825.33	3872.0			
Yoke	4125.33	7426.33	4047.0	Yoke_symmetry	12	
YokeEndcap	300.0	7426.33	4072.0, 7373.0	YokeEndcap_symmetry	12	
YokeEndcapPlug	300.0	3045.83	3937.2, 4072.0	YokeEndcapPlug_symmetry	12	
BeamCal	17.8	140.0	3115.0, 3315.024	BeamCal_thickness	220.03	
LHCal	130.0	315.0	2680.0, 3160.0	LHCal_thickness	480.0	
LumiCal	80.0	202.09	2411.8, 2540.5	LumiCal_thickness	128.7	

Compare with

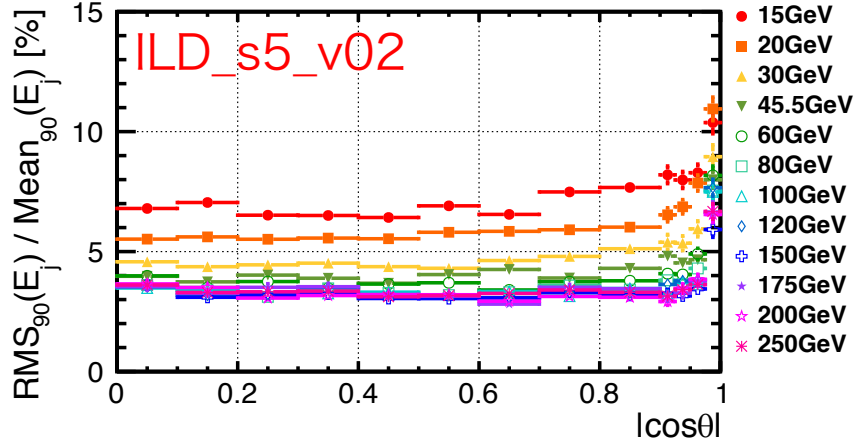
sv01-19-05 $|\cos\theta| < 0.7$



sv01-19-05.mILD_I5_o1_v02_nobg



sv01-19-05.mILD_s5_o1_v02_nobg



エネルギー分解能の定義

$$\frac{\sigma_{E_j}}{E_j} = \frac{\text{RMS}_{90}(E_j)}{\text{mean}_{90}(E_j)} = \sqrt{2} \frac{\text{RMS}_{90}(E_{jj})}{\text{mean}_{90}(E_{jj})}$$

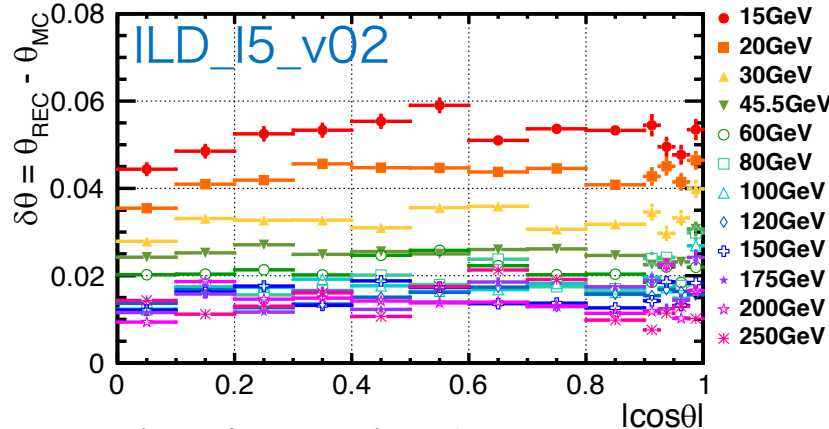
RMS₉₀

ヒストグラム内の90%の事象が含まれる
最小の領域における標準偏差を用いる

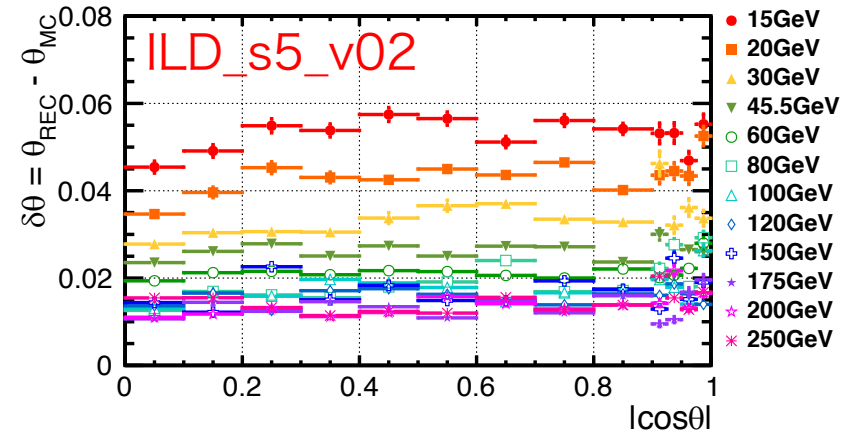
極角分解能

$$\delta\theta = RMS_{90}(\theta_{rec} - \theta_{mc})$$

sv01-19-05.mILD_I5_o1_v02_nobg

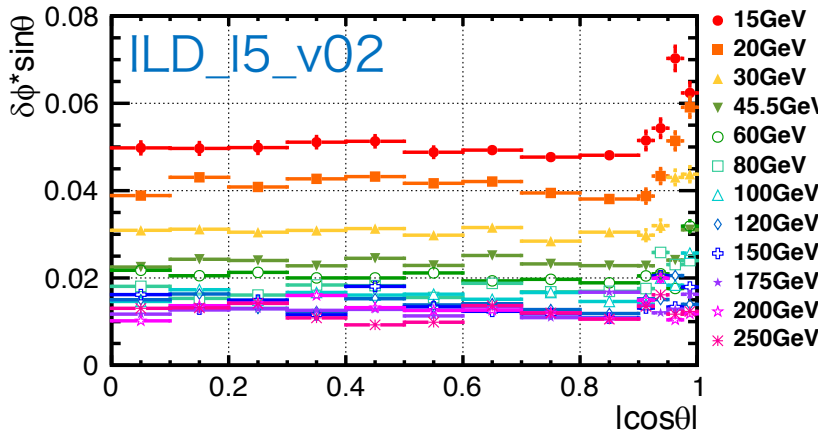


sv01-19-05.mILD_s5_o1_v02_nobg

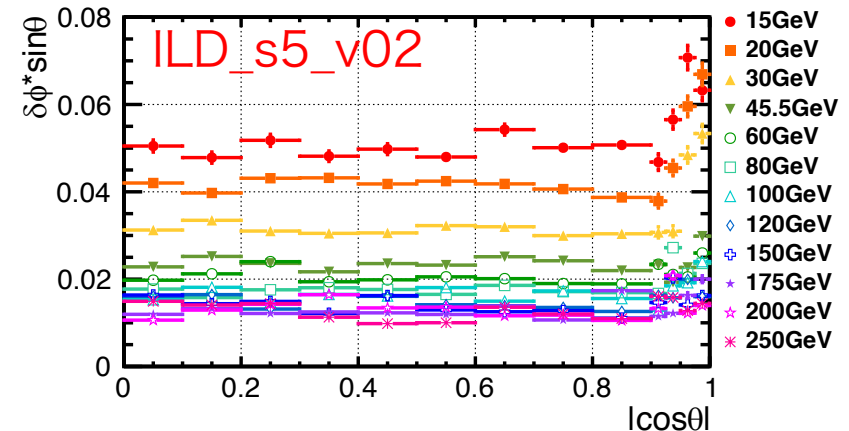


方位角分解能 $\delta\phi * sin\theta = RMS_{90}\{(\phi_{rec} - \phi_{mc})sin\theta\}$

sv01-19-05.mILD_I5_o1_v02_nobg



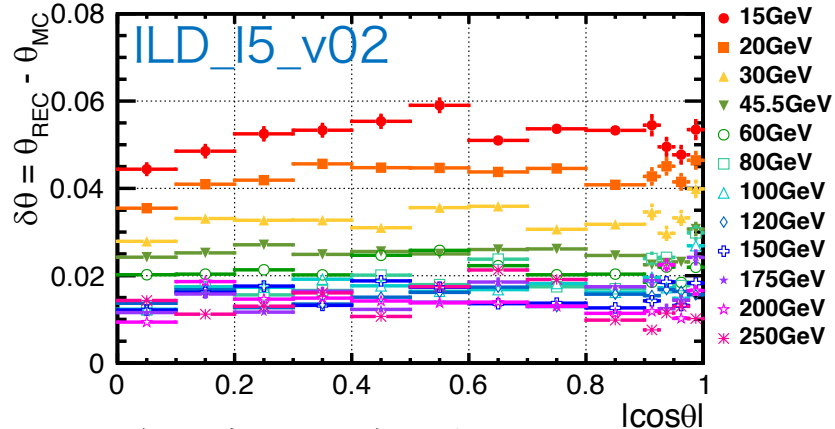
sv01-19-05.mILD_s5_o1_v02_nobg



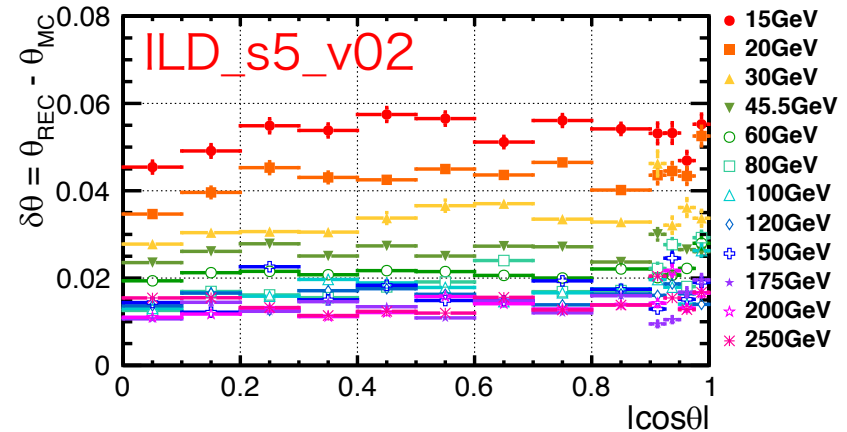
極角分解能

$$\delta\theta = RMS_{90}(\theta_{rec} - \theta_{mc})$$

sv01-19-05.mILD_I5_o1_v02_nobg



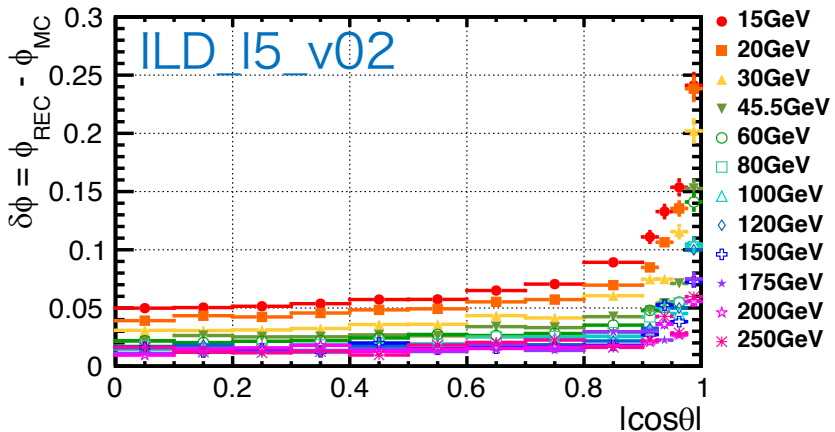
sv01-19-05.mILD_s5_o1_v02_nobg



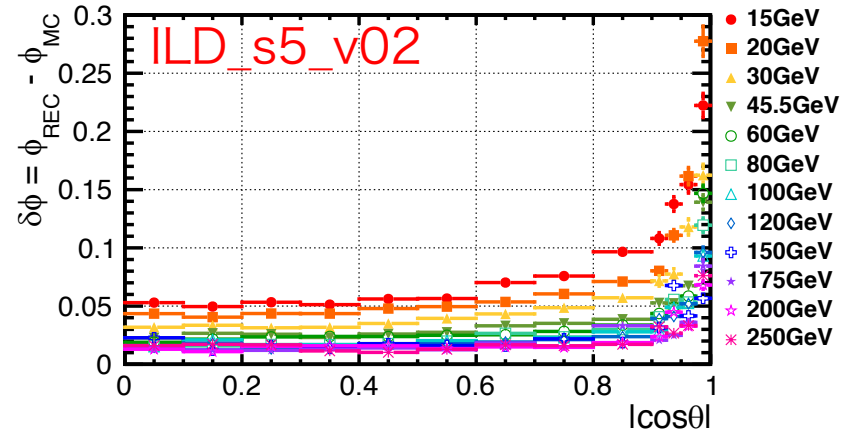
方位角分解能

$$\delta\phi = RMS_{90}(\phi_{rec} - \phi_{mc})$$

sv01-19-05.mILD_I5_o1_v02_nobg



sv01-19-05.mILD_s5_o1_v02_nobg



Event Selection

1. isolated lepton veto
2. loose restriction
[transverse di-jet momentum, di-jet invariant mass, recoil mass from di-jet]
3. number of PFOs and charged tracks: N_{pfo} , N_{track}
4. di-jet (Z) pt: Pt_Z
5. di-jet mass: M_Z
6. di-jet polar angle: θ_Z
7. recoil mass: M_{recoil}
8. multi-variate analysis: Boosted Decision Tree(BDT) method

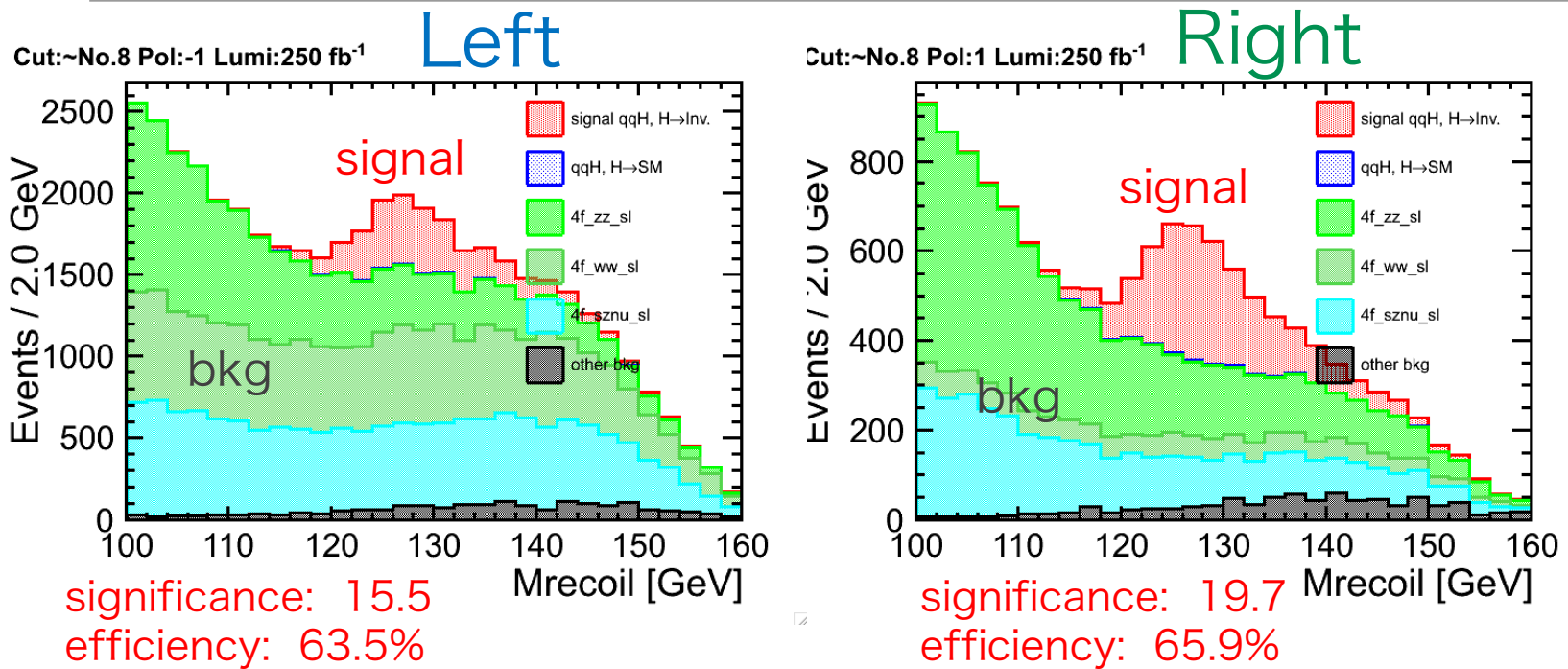
生成断面積とモンテカルロサンプル

サンプル名	生成断面積 [fb ⁻¹]		生成事象数	
	左完全偏極	右完全偏極	左完全偏極	右完全偏極
qqH, H → inv. (BR = 10%)	34.6	22.2	19701	19900
qqH (SM)	346.0	222.0	346336	222351
ZZ semi-leptonic	1422.1	713.5	356461	178635
WW semi-leptonic	18781.0	172.7	1919148	43501
$\nu\nu Z$ semi-leptonic	456.8	130.8	114516	32998
other bkg	223851	114716	17312470	

左完全偏極 : $(P_{e^-}, P_{e^+}) = (-1.0, +1, 0)$

右完全偏極 : $(P_{e^-}, P_{e^+}) = (+1.0, -1, 0)$

反跳質量分布 [Ecm = 250 GeV, 250 fb⁻¹, BR(H→inv.)=10%]



MVA input variables	
di-jet inv. mass	one jet polar angle
di-jet polar angle	another jet polar angle

TMVA v-4.2.0

No.	Cut	No.	Cut
1	Isolated lepton veto	5	80 < di-jet invariant mass < 100
2	Loose Cut (Pt _z , M _z , M _{recoil})	6	di-jet polar angle < 0.9
3	#pfo > 15 & #all_track > 6 & # track_in_one_jet > 1	7	100 < recoil mass < 160
4	20 GeV < di-jet Pt < 80 GeV	8	BDT cut

崩壊分岐比 95% CL 上限の推定

● テンプレート法

1. $\text{BR}(\text{H} \rightarrow \text{invisible}) = \mu = [1, 2, \dots, 10]\%$ でモンテカルロ生成
2. 事象選別を行う
3. $N_{S+B}(\mu)$ ($M_{\text{recoil}} \in [120, 140] \text{ GeV}$) を取得
4. $N_{S+B}(\mu)$ のポアソン分布を生成 \rightarrow 95% CL の下限値 N_{UL} を取得
5. $\mu = [1, 2, \dots, 10]\%$ について 1~3 を行う $\rightarrow \mu$ vs N_{UL} の較正直線を作成
6. 実際の実験結果に対して、事象選別の後 $M_{\text{recoil}} \in [120, 140] \text{ GeV}$ の事象数を取得 \rightarrow 較正直線で崩壊分岐比 95% CL 上限に変換

手順6の実験結果に相当するものとして

標準理論想定、つまりシミュレーションで得た背景事象のみの分布を用いる

